Probing the Molecule−Electrode Interface of Single-Molecule Junctions by Controllable Mechanical Modulations

Jianfeng Zhou, Guojun Chen, and Bingqian Xu*

Molecular Nanoelectronics, Faculty of Engineering & Nanoscale Science and Engineering Center, University of Georgia, Athens, Georgia 30602

Received: February 9, 2010; Revised Manuscript Received: March 16, 2010

Presented here is an in-depth study to exploit the molecule−electrode interface effects on electronic transport properties in stabilized molecular junctions under controlled mechanical modulations. By monitoring and analyzing the conductance and force changes corresponding to the modulations, we *isolated* the effects of both the molecule terminating groups and the different contact configurations on electronic transport properties. The experimental results can be understood by our calculations developed based on simple and straightforward models. The results would be helpful not only to resolve the discrepancies of the recent scanning tunneling microscopy molecular break junction experiment results but also to add new insights into the understanding of the electronic transport mechanisms of molecular junctions.

Introduction

The ultimate goal of molecular electronics is to use functional electronic devices made from single molecules.[1−4] As a prerequisite to achieving this goal, it is crucial to be able to measure, control, and understand the electronic transport properties of such molecular devices.[5,6] Studies have shown that, in a molecular junction, one of the most intensively studied molecular devices, the electronic transport characteristics are determined by not only the molecular core but also the features of metal−molecule interfaces.[6−9] The molecular core depends on what and how the atoms make up the molecule, while the issue of interface includes the chemical nature and the contact geometric configurations[10−14] of the interface atom, which is much more complex, and thus, little has been known about many behaviors of the interface.[15] The main reason for the current difficulties first lies in the fact that many factors in the molecule−electrode interface can contribute to the transport properties; these factors include contact stabilities of molecular junctions,[16,17] contact bond length,[18] contact bond angles,[19] terminating anchoring group of molecule to electrode,[20−22] the arrangement of electrode atom,[23,24] and so on. Second, these interface factors couple with each other to make it difficult to identify their distinct influences on electron transport through molecules. Moreover, the difficulties are aggravated by a lack of effective experimental methods to monitor and control the microstructures of contact geometric configurations. In the previous experimental and theoretical results,[21,25−28] even for the simplest single molecule, it shows several orders variation of single molecular conductance values because of the less control over the contact configurations.[12,29] Therefore, the experimental methods that can be used to isolate the effects of the interfaces on electronic transport properties are expected urgently to result in a deeper understanding of the electronic transport properties in molecular junctions.

In this article, we report an in-depth study of electronic transport properties of Au−alkanedithiol/alkanediamine−Au junctions, focusing on metal−molecule interface effects: both the terminating anchoring group of the molecule to the electrode and the contact configurations. Our earlier study revealed multiple conductance values of single-molecule junctions corresponding to specific stable contact configurations.[30] Here, we monitor and analyze the conductance and force changes corresponding to the modulating of the contact configurations of a specific stable contact configuration by introducing mechanical perturbations.[8,19,31] Regular ac triangular piezoelectric transducer (PZT) modulations are applied as controllable perturbations[8] in the free-holding processes of the modified scanning probe microscopy break junction technique (SPMBJ).[30] On the basis of the responsive conductance and force signals monitored simultaneously, we aim to build the connection among the conductance fluctuations, force changes, and the PZT modulations. The results would be helpful not only to resolve the discrepancies of the recent STM break junction experiment results but also to add new insights into the understanding of the electronic transport mechanisms of molecular junctions.

Experimental Section

Chemicals and Materials. 1,8-octanedithiol ($HS(CH_2)_8SH$) and 1,8-octanediamine ($H_2N(CH_2)_8NH_2$) were purchased from Aldrich. Other solvents were used directly as received.

Au(111) Substrate Preparation. Gold substrates were prepared by evaporating ∼100 nm of gold onto freshly cleaved mica sheets using an evaporator under a vacuum of 10^{-7} Torr. The gold beads for Au substrate deposition come from Kurt J. Lesker Company (99.999%), and mica sheets were from Ted Pella, Inc. The surfaces were annealed in a hydrogen flame immediately before immersion in sample solutions. This annealing step cleans the surface and allows epitaxial reconstruction of the Au to form large terraces of Au(111).

Preparation of Self-Assembly Monolayers (SAMs). C8DT SAMs on gold substrates were prepared by soaking the 1 mM solution of C8DT toluene solution for 3 h. The C8DT molecules formed compact packed monolayers. C8DA SAMs on gold were prepared by soaking the 1 mM solution of C8DT water solution for 3 h. The coated gold substrates were then rinsed in the water solution three times and put in pure toluene after drying with argon.

* To whom correspondence should be addressed. E-mail: bxu@engr.uga.edu.

10.1021/jp101257y
Published on Web 04/02/2010

Experimental Setup and Data Analysis. The SPM setup is the PicoPlus SPM system (Molecular Imaging) using a Pico Scan 3000 Controller (Molecular Imaging). The conducting AFM tip was made of Si (Nanoscience Instruments) coated with a 15 nm layer of chromium and then a 35 nm layer of gold (99.999%) using an ion beam coater (Gatan model 681) before each measurement. The spring constant of the AFM cantilever was calibrated to be around 40 N/m. To minimize the contamination from the external environment, the measurements were performed using a Teflon cell mounted inside of a glass chamber flashed with N_2. Before each experiment, the cell was cleaned by boiling it in piranha solution (98% H_2SO_4/30% H_2O_2, 3:1, v/v) and then was thoroughly sonicated in 18 MΩ water three times (Barnstead NanopureDiamond system fed with DI water) (Caution: piranha solution reacts violently with most organic materials and must be handled with extreme care). The modified SPM break junctions and regular modulation are realized by controlling the movement of the PZT, and experiment data were acquired and analyzed by using our homemade Labview computer programs.

Results and Discussion

The principles of our method are based on the modified SPMBJ technique, as shown in Figure 1. The Au STM tip or Au-coated conducting AFM tip was brought in contact into and out of the Au (111) substrate coated with molecular self-assembly monolayers (SAMs). The bias voltage applied throughout the experiments is 0.3 V. In contrast with the traditional SPM break junction technique[32] (Figure 1a, inset, A), we divided the continuous tip retracting process into sharply stretching and free-holding processes (Figure 1a, inset, B).[30] After abruptly stretching about 1 nm, the current and force signals are recorded during which the molecules are kept free-holding between two electrodes. With the modified SPMBJ technique, the complexities of contact conformation changes, caused by the continuous SPM tip movement during the retracting process, have been minimized.[30] During the free-holding process to regulate the distance between the two electrodes, a triangular wave signal with a certain frequency (fixed at 240 Hz in all the experiments) and amplitude was applied (Figure 1a, inset, C). During the modulation, the molecules used in our work, ocanedithiol(C8DT) and ocanediamine (C8DA), can be considered as a rigid body because of the much stronger covalent C−C bonds in the molecule than S−Au, NH_2−Au, and Au−Au bonds in the contacts.[33] Therefore, most of the changes in conductance introduced by the modulations should come from the corresponding changes of the molecule−electrode contact interface. The representative conductance trace (Figure 1b) shows out-of-phase correspondence to the PZT modulation signals. The correspondent force changes caused by PZT modulation are also recorded simultaneously (Figure 1b).

Simply speaking, without modulation, the molecular junction was stabilized by free-holding with the molecule sandwiched between electrodes, with the contact potential barrier E_0. When the PZT signal is at the peak under modulation, the SPM tip is farthest away from the substrates with the stretching displacement increment Δz. The stretching force F goes to the maximum value so that the contact potential barrier increases to its maximum $E_0 + F\Delta z$, resulting in the largest contact resistance. As a result, the conductance of the molecular junction would be reduced to the minimum value. Oppositely, when the PZT signal goes to the valley, the conductance value increases to the maximum due to the decreased contact potential barrier, as shown in Figure 1b. Similar phenomena have been suggested by the theoretical calculations[18] and observed in our previous experiments.[8]

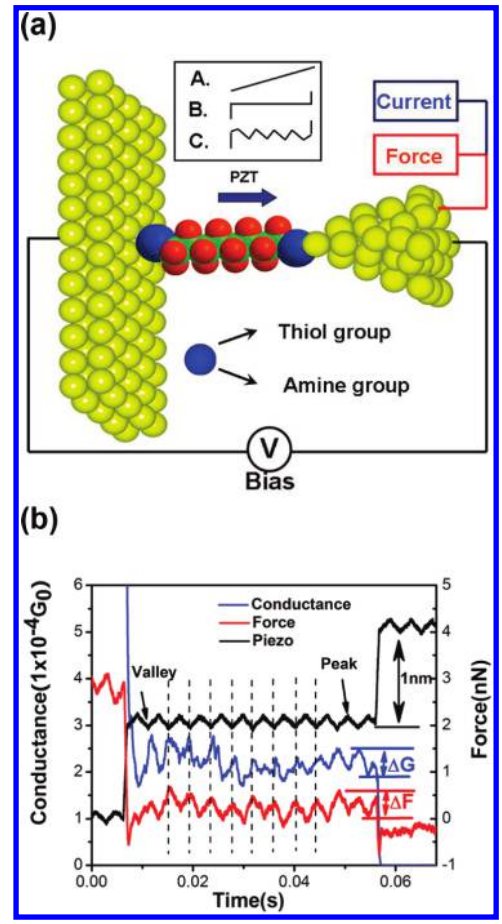

Figure 1. (a) The schematics of the SPM break junction technique. The inset shows the SPM tip retracting modes driven by PZT: (A) traditional SPM break junction technique with SPM tip continuously retracting, (B) modified SPM break junction technique with sharp withdrawal and free-holding process, and (C) regular modulations applied during the free-holding process with the modified SPM break junction technique. The current and force signals were measured and recorded simultaneously. (b) Typical conductance and force traces for C8DT with PZT modulation (black). The arrows label the maximum (peak) and minimum (valley) positions of PZT modulation signals. The corresponding conductance change ΔG (blue) and the force fluctuation amplitude ΔF (red) are labeled as shown.

Thorough analysis of the recorded traces obtained in the experiments reveals several new specific characteristic features for C8DA and C8DT molecular junctions (Figure 2). First, in the conductance traces with plateaus (35−60% for C8DA and 45−70% for C8DT under different modulation amplitudes), indicating the formation of stabilized molecular junctions, over 40% of the traces show perfect correspondence of force and conductance to the modulation signals for both molecules (as shown by the dashed vertical lines in Figure 2a,b). Second, some conductance traces show conductance switching between different conductance sets that were reported in our previous report[30] (Figure 2c) without an obvious force change. A possible explanation could be the switching between the stable states of the contact configurations of the molecular junction stimulated by the PZT modulations. As the calculations of Stoltze[34] and Boisvert[35] suggest, the Au atom diffusion energy on the Au(111) surface is between 0.1 and 0.2 eV, much smaller than the binding energy E_b of Au−Au, 0.84 eV,[17] and the Au−NH_2 binding energy, 0.71 eV.[36] Therefore, under the PZT modulations, the shear component of the force was applied on Au atoms in the contact parts, caused by stretching or compressing the molecular junctions. The Au atoms can be activated to switch

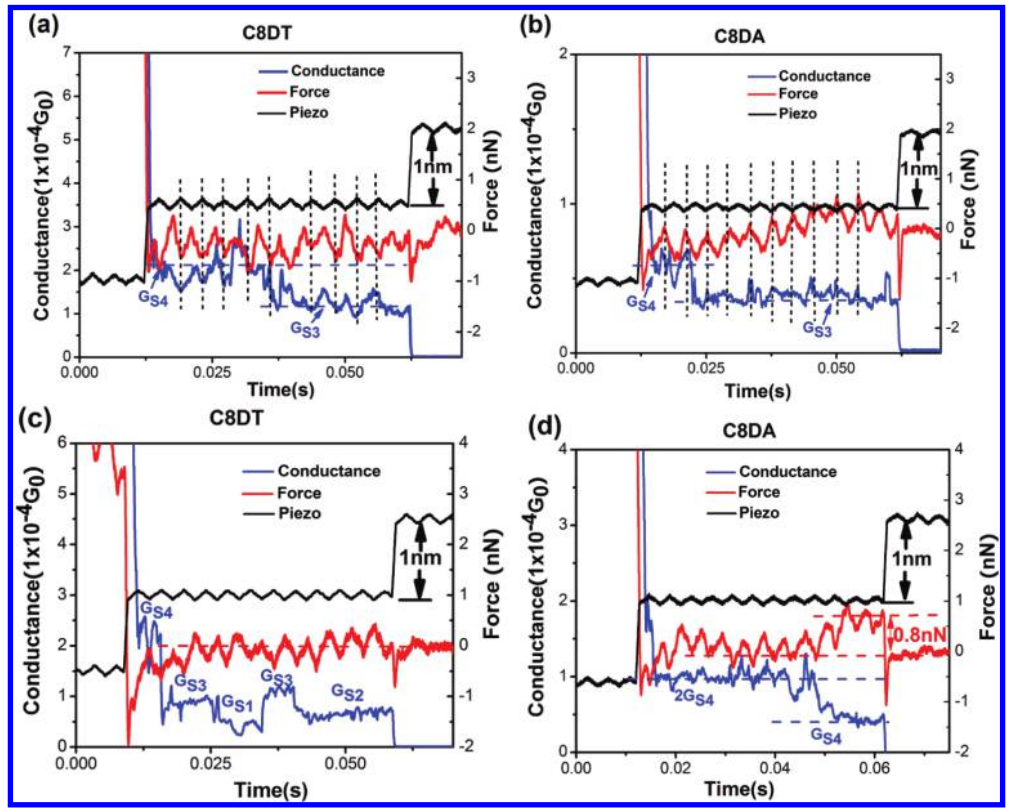

Figure 2. Representative traces indicating various specific characteristic features. The force and conductance traces show out-of-phase (180° phase shift) correspondence to the modulation for both (a) C8DT and (b) C8DA. (c) The trace with conductance switching between different single molecular conductance sets under modulations. (d) The trace with conductance changes with dissociations of molecules from electrodes caused by the contact bond broken, G_{S1}−G_{S4} (C8DT, 4.8×10^{-5}, 7.0×10^{-5}, 9.0×10^{-5}, and 24.9×10^{-5} G_0) in (c) and G_{S4} (C8DA, 5.2×10^{-5} G_0) in (d) are the single molecular conductance sets reported in our previous work.[30]

between different adsorption sites by this shear component. This switching movement would not introduce tremendous force changes as in bond breaking.

Remarkably, in addition to the switching between different stable conductance sets, for C8DA, another specific feature was identified. As is shown in Figure 2d, two conductance steps appear in one free-holding process under the modulation and the conductance at the higher step is two times that of the lower one, which are accompanied with a force change of 0.7−0.9 nN, close to the Au−NH_2 binding force.[33] The phenomena strongly suggest that the responsive conductance changes are a combination of the switching between different adsorption sites and the dissociation of the molecule from the electrode with the bond broken under modulations. Especially, in the entire conductance traces with C8DA molecular junctions formed (>500 traces for each amplitude), the ratio of the traces with this bond breaking increases remarkably with modulation amplitude (Figure 3a). Without modulation, the ratio is less than 2% and goes to 38% with 0.12 nm modulations. Within the range of the applied modulation forces, bond breaking was never observed for C8DT.

To understand the observed new specific features about the molecule−electrode contact interfaces, we discuss the contact stabilities of molecular junctions by calculating their lifetimes under different modulation amplitudes. As is known, the lifetime equation of a chemical bond under external force is[37,38]

$$\tau_F = \tau_D \exp\left(\frac{E_b - F\chi}{k_B T}\right) = \tau_{off} \exp\left(-\frac{F\chi}{k_B T}\right) \quad (1)$$

where τ_D is the diffusion relaxation time, E_b is the binding energy, k_BT is 4 pN·nm at room temperature, τ_{off} is the natural lifetime of molecular junctions without external force, and $F\chi$ is the work done by the external force along the bond elongation direction. To obtain the $F\chi$ in our system, we constructed the histogram using force modulations to get the average force fluctuations ΔF under different modulation amplitudes ΔA (Figure 3b). The ΔF of each circle of the modulation on the force curves (about 200 curves were used for each modulation amplitude applied) was recorded using a homemade Labview computer program, as is shown in the inset in Figure 3b, for $\Delta A = 0.08$ nm as an example. It is important to notice that, even without adding any modulation, there are still force fluctuations due to the spontaneous phonon fluctuations and mechanical vibration of the system (Figure 3b). Under small modulation in our experiments, the force modulation ΔF increases linearly with the stretching distances, and under the same modulations, the force modulations for both C8DA and C8DT are found to be very similar in amplitudes. In consideration of the triangular modulations, only the force to stretch the molecular junctions and displacement along the stretching direction would mainly contribute to the breaking of the contact bond and the effective work is half the product of maximal force and displacement. Therefore, the average effective work to lower the contact binding energy caused by the modulations was estimated as

$$F\chi = \frac{1}{2}\left(\frac{1}{2}\Delta F\right)\left(\frac{1}{2}\Delta A\right) = \frac{1}{8}\Delta F \Delta A \quad (2)$$

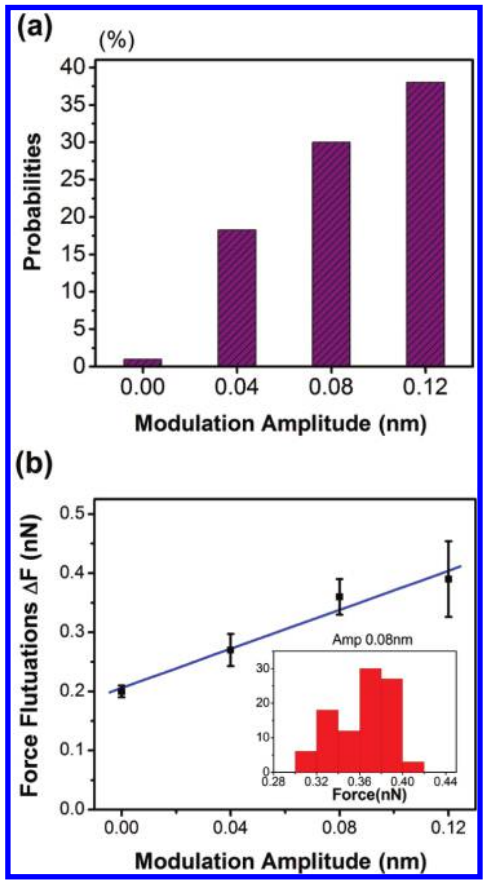

Figure 3. (a) The probabilities of the traces with the bond broken under different modulation amplitudes. (b) The most probable force fluctuations obtained by constructing histograms of the force fluctuations value using ~200 traces under different modulation amplitudes (inset of (b) shows the force fluctuation values (around 200 trances) at a 0.08 nm modulation amplitude). The blue line is the linear fitting for the force change versus modulation amplitude.

TABLE 1: Lifetimes of C8DT and C8DA at Different Modulation Amplitudes

	N/A	amp 0.04 nm	amp 0.08 nm	amp 0.12 nm
C8DT (s)	8.00	5.78	3.59	2.00
C8DA (s)	0.20	0.14	0.09	0.05

By introducing this average effective work (eq 2) into eq 1, we can obtain the lifetimes for C8DA and C8DT under modulations (Table 1). As is reported,[36] the molecular junctions with two thiol anchoring groups are always broken at the weaker Au−Au bond whose ideal natural lifetime τ_{off} is about 8 s, whereas the molecular junctions with two amine terminal anchoring groups are always broken at the weaker Au−amine bond whose natural lifetime τ_{off} is only 0.2 s. For C8DT, even though the modulation amplitude goes to 0.12 nm, the lifetime would still be around 2 s, much longer than our 50 ms free-holding period. In sharp contrast, when the modulation amplitude increases, the lifetime of C8DA molecular junctions becomes very close to the 50 ms free-holding period. Therefore, even with wide distributions of lifetime, under modulation, there are always much more C8DA molecular junctions whose lifetime would become shorter than the free-holding period than C8DT molecular junctions where this probability is much smaller. Under relatively larger modulations (>0.15 nm), the molecular junctions became increasingly unstable and eventually no stable junctions could be formed. Our results also agree with previous reports,[36] indicating that the molecular junctions with thiol−Au contact bonds are more stable than the molecular junctions with amine−Au contact bonds. The discussions here were based on the simple and rigid molecules that were held stably between two solid electrodes with the SPM break junction technique. In those cases, the configuration changes in other dimensions except for the pulling coordinate, can be neglected during the modulation process. If more complex molecular structures were involved, the multidimensional dynamic effects may need to be considered as proposed by recent reports.[39]

The contact configuration changes introduced by modulations not only impact the stabilities of molecular junctions but also have significant influences on the electron transport efficiency of single-molecule junctions. As is known, the electronic transport through saturated molecules of alkanes, which have rather large HOMO−LUMO gaps, is electron tunneling[30,32,40]

$$G_L = D_0 \exp(-\beta_L L) \tag{3}$$

where β_L is the decay constant of the molecule itself and L is the length of the molecule. D_0 is the constant related to the contact resistance. When we introduce the modulations, as is discussed above, the length increment Δz mostly becomes the contact part. Therefore, we introduce here the contact decay constant β_C, which should be different from that of the molecule itself and represents the effect of different contact configurations. The conductance with modulations (G_M) can still be described as[41]

$$G_M = D_0 \exp(-\beta_L L - \beta_C \Delta z) = G_L \exp(-\beta_C \Delta z) \tag{4}$$

under the modulation with small amplitude ΔA

$$\frac{\Delta G_M}{G_L} = \left(\exp\left(\frac{1}{2}\beta_C \Delta A\right) - \exp\left(-\frac{1}{2}\beta_C \Delta A\right)\right) = 2\sinh\left(\frac{1}{2}\beta_C \Delta A\right) \cong \beta_C \Delta A \tag{5}$$

For the average relative conductance fluctuation amplitude $\Delta G/G$, we also have to include the relative conductance changes $\Delta G_V/G_L$ introduced by spontaneous thermal fluctuation and mechanical vibrations of the system. Therefore

$$\frac{\Delta G}{G} = \frac{\Delta G_M}{G_L} + \frac{\Delta G_V}{G_L} \cong \beta_C \Delta A + \frac{\Delta G_V}{G_L} \tag{6}$$

In our previous report,[30] there are four single molecular conductance sets observed for each of C8DA and C8DT due to different contact configurations. As is shown in eq 4, the contact decay constant β_C can be used as a significant index to identify the different contact configurations of molecular junctions. By doing the linear fitting for the relationship between $\Delta G/G$ and the modulation amplitude ΔA (Figure 4a,b), we can obtain the β_C values and $\Delta G_V/G_L$ for each preferential contact configurations of C8DA and C8DT molecular junctions (Table 2). $\Delta G_V/G_L$ can also be obtained just by direct measurement of the conductance fluctuation amplitudes without modulations. The fitting results and measured values of $\Delta G_V/G_L$ for different conductance sets of C8DA and C8DT have been compared (insets of Figure 4a,b). The values are very close to each other, indicating that the linear fitting provides the satisfactory

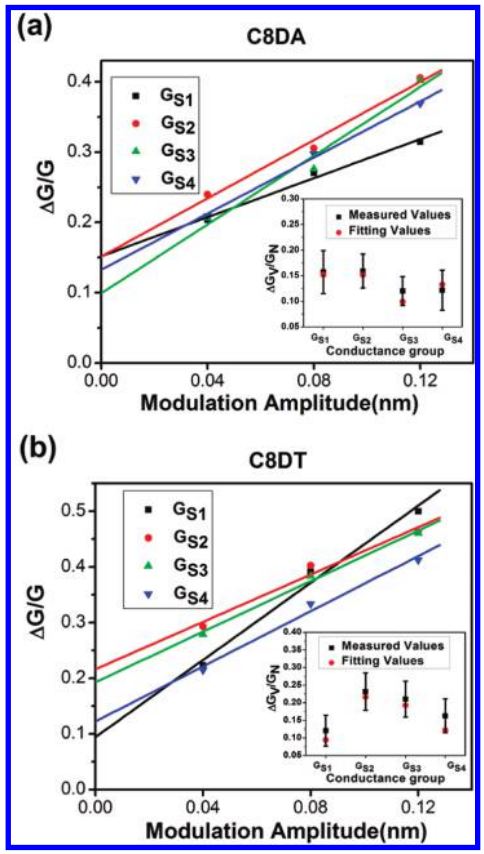

Figure 4. Linear fitting for relative conductance fluctuation amplitude versus modulation amplitude for C8DA (a) and C8DT (b). The different conductance sets are labeled with different colors. The insets compare the fitting $\Delta G_V/G_L$ (red) values and the measured $\Delta G_V/G_L$ (black) values.

TABLE 2: Fitting β_C and $\Delta G_V/G_L$ Values for Different Contact Conformations in Figure 4

	C8DA		C8DT	
	β_C	$\Delta G_V/G_L$	β_C	$\Delta G_V/G_L$
G_{S1}	1.39	0.152	3.46	0.094
G_{S2}	2.10	0.151	2.13	0.216
G_{S3}	2.44	0.099	2.27	0.193
G_{S4}	1.99	0.133	2.47	0.122

approximation for our discussions. The fitting β_C values are much smaller than the decay constant of the molecule itself (6−8/nm).[31] The results also confirm our assumption that the modulations mainly cause the changes of contact configuration and, therefore, result in conductance changes. The molecules are relatively kept intact.

As is discussed above, the conductance changes under modulation result from contact potential barrier fluctuations caused by the forces applied. Therefore, we can build the direct relationship between conductance changes and the force changes. In our case, the force changes ΔF and modulations amplitude ΔA have a linear relationship, as shown in Figure 3b

$$\Delta A = \frac{\Delta F - \Delta F_0}{k} \tag{7}$$

where $k = 1.65$ nN/nm is the slope and $\Delta F_0 = 0.206$ nN, the force fluctuations caused by the spontaneous thermal fluctuations and mechanical vibration of the system, is the intercept of fitting line. Therefore, the relative conductance fluctuation amplitudes follow the equation

$$\frac{\Delta G}{G} \cong \beta_C \frac{\Delta F - \Delta F_0}{k} + \frac{\Delta G_V}{G_L} \tag{8}$$

Under small modulation in our study, for each set of the conductance corresponding to a stable contact configuration, the relative conductance fluctuation amplitude increases linearly with the force change. However, conductance fluctuation amplitude of different sets of the conductance under the same force are different (Figure 4). This is because contact configurations cause different contact potentials, the effect of which on conductance can be expressed by different contact decay constants β_C (Table 2). The results of this study also provide a possible way to tune the electron transport through molecular junctions by mechanical methods to modify the contact configurations.

Conclusions

In summary, we introduced, in this study, controllable mechanical modulations to tune the contact configurations of C8DA and C8DT molecular junctions based on the modified SPM break junction methods. By monitoring the responsive conductance fluctuations and force changes simultaneously, we investigated the influences of contact configuration changes on electron transport properties of molecular junctions. The molecular junctions were found to become severely unstable by mechanical modulations even at small amplitude. Also, as is shown in our experimental results, the stabilities of C8DA are much less than those of the C8DT, which is in good agreement with previous reports and our calculations.

We established a simple analysis to identify the crucial factors that affect the electronic transport in single-molecule junctions introduced by the modulations. Our experimental results agree well with the simple theoretical calculation results based on ideal models. The contact decay constant β_C, the significant quantity to identify the different contact configurations, can be obtained by analyzing the linear relationship between relative conductance fluctuations and the modulation amplitudes. β_C is smaller than, and independent of, the molecular decay constant β_L, suggesting that the modulations were indeed applied to the contact part but not to the molecule itself. We also deduced an equation to connect relative conductance fluctuation amplitudes with the force changes. The results of this study proposed a potential way to tune the electron transport properties with mechanical methods.

Acknowledgment. We gratefully acknowledge the National Science Foundation (ECCS 0823849) for financial support.

References and Notes

(1) Aviram, A.; Ratner, M. *Chem. Phys. Lett.* **1974**, *29*, 277.
(2) Nitzan, A.; Ratner, M. A. *Science* **2003**, *300*, 1384.
(3) Service, R. F. *Science* **2001**, *294*, 2442.
(4) Tao, N. J. *Nat. Nanotechnol.* **2006**, *1*, 173.
(5) Bumm, L. A.; Arnold, J. J.; Cygan, M. T.; Dunbar, T. D.; Burgin, T. P.; Jones, L.; Allara, D. L.; Tour, J. M.; Weiss, P. S. *Science* **1996**, *271*, 1705.
(6) Lindsay, S. M.; Ratner, M. A. *Adv. Mater.* **2007**, *19*, 23.
(7) Nitzan, A. *Annu. Rev. Phys. Chem.* **2001**, *52*, 681.
(8) Xu, B. Q. *Small* **2007**, *3*, 2061.
(9) Xue, Y. Q.; Ratner, M. A. *Phys. Rev. B* **2004**, *69*, 161402.
(10) Nara, J.; Geng, W. T.; Kino, H.; Kobayashi, N.; Ohno, T. *J. Chem. Phys.* **2004**, *121*, 6485.

(11) Wu, X.; Li, Q.; Huang, J.; Yang, J. *J. Chem. Phys.* **2005**, *123*, 184712.
(12) Bilić, A.; Reimers, J. R.; Hush, N. S. *J. Chem. Phys.* **2005**, *122*, 094708.
(13) Kondo, H.; Kino, H.; Nara, J.; Ozaki, T.; Ohno, T. *Phys. Rev. B* **2006**, *73*, 235323.
(14) Li, X.; He, J.; Hihath, J.; Xu, B.; Lindsay, S. M.; Tao, N. *J. Am. Chem. Soc.* **2006**, *128*, 2135.
(15) Ulrich, J.; Esrail, D.; Pontius, W.; Venkataraman, L.; Millar, D.; Doerrer, L. H. *J. Phys. Chem. B* **2006**, *110*, 2462.
(16) Tsutsui, M.; Shoji, K.; Taniguchi, M.; Kawai, T. *Nano Lett.* **2008**, *8*, 345.
(17) Huang, Z.; Chen, F.; Bennett, P. A.; Tao, N. *J. Am. Chem. Soc.* **2007**, *129*, 13225.
(18) Andrews, D. Q.; Duyne, R. P. V.; Ratner, M. A. *Nano Lett.* **2008**, *8*, 1120.
(19) Quek, S. Y.; Kamenetska, M.; Steigerwald, M. L.; Choi, H. J.; Louie, S. G.; Hybertsen, M. S.; Neaton, J. B.; Venkataraman, L. *Nat. Nanotechnol.* **2009**, *4*, 230.
(20) Yasuda, S.; Yoshida, S.; Sasaki, J.; Okutsu, Y.; Nakamura, T.; Taninaka, A.; Takeuchi, O.; Shigekawa, H. *J. Am. Chem. Soc.* **2006**, *128*, 7746.
(21) Chen, F.; Li, X.; Hihath, J.; Huang, Z.; Tao, N. *J. Am. Chem. Soc.* **2006**, *128*, 15874.
(22) Venkataraman, L.; Klare, J. E.; Tam, I. W.; Nuckolls, C.; Hybertsen, M. S.; Steigerwald, M. L. *Nano Lett.* **2006**, *6*, 458.
(23) Müller, K.-H. *Phys. Rev. B* **2006**, *73*, 045403.
(24) Lee, M. H.; Speyer, G.; Sankey, O. F. *Phys. Status Solidi B* **2006**, *243*, 2021.
(25) Engelkes, V. B.; Beebe, J. M.; Frisbie, C. D. *J. Am. Chem. Soc.* **2004**, *126*, 14287.
(26) Cui, X. D.; Primak, A.; Zarate, X.; Tomfohr, J.; Sankey, O. F.; Moore, A. L.; Moore, T. A.; Gust, D.; Nagahara, L. A.; Lindsay, S. M. *J. Phys. Chem. B* **2002**, *106*, 8609.
(27) Akkerman, H. B.; de Boer, B. *J. Phys.: Condens. Matter* **2008**, *20*, 013001.
(28) Haiss, W.; Nichols, R. J.; van Zalinge, H.; Higgins, S. J.; Bethell, D.; Schiffrin, D. J. *Phys. Chem. Chem. Phys.* **2004**, *6*, 4330.
(29) Ramachandran, G. K.; Hopson, T. J.; Rawlett, A. M.; Nagahara, L. A.; Primak, A.; Lindsay, S. M. *Science* **2003**, *300*, 1413.
(30) Zhou, J.; Chen, F.; Xu, B. *J. Am. Chem. Soc.* **2009**, *131*, 10439.
(31) Xia, J. L.; Diez-Perez, I.; Tao, N. J. *Nano Lett.* **2008**, *8*, 1960.
(32) Xu, B.; Tao, N. J. *Science* **2003**, *301*, 1221.
(33) Xu, B. Q.; Xiao, X. Y.; Tao, N. J. *J. Am. Chem. Soc.* **2003**, *125*, 16164.
(34) Stoltze, P. *J. Phys.: Condens. Matter* **1994**, *6*, 9495.
(35) Boisvert, G.; Lewis, L. J.; Puska, M. J.; Nieminen, R. M. *Phys. Rev. B* **1995**, *52*, 9078.
(36) Tsutsui, M.; Taniguchi, M.; Kawai, T. *J. Am. Chem. Soc.* **2009**, *131*, 10552.
(37) Evans, E.; Ritchie, K. *Biophys. J.* **1997**, *72*, 1541.
(38) Evans, E. *Annu. Rev. Biophys. Biomol. Struct.* **2001**, *30*, 105.
(39) Suzuki, Y.; Dudko, O. K. *Phys. Rev. Lett.* **2010**, *104*, 048101.
(40) Wold, D. J.; Frisbie, C. D. *J. Am. Chem. Soc.* **2001**, *123*, 5549.
(41) York, R. L.; Nguyen, P. T.; Slowinski, K. *J. Am. Chem. Soc.* **2003**, *125*, 5948.

JP101257Y